

1 McCormick Relaxation

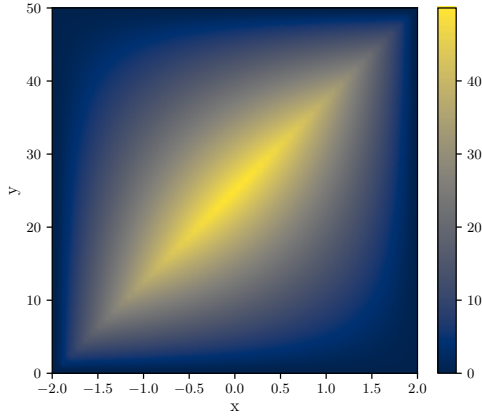
To address bilinear terms of the form $w = xy$, we introduce the following constraints based on the bounds of x and y :

$$x^L \leq x \leq x^U, \quad y^L \leq y \leq y^U.$$

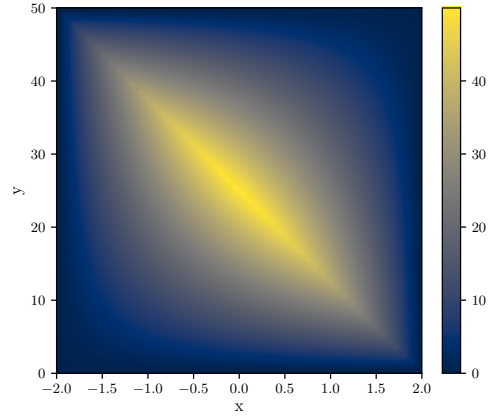
The resulting McCormick relaxation constraints for w are:

$$\begin{aligned} w &\geq x^L y + xy^L - x^L y^L, \\ w &\geq x^U y + xy^U - x^U y^U, \\ w &\leq x^U y + xy^L - x^U y^L, \\ w &\leq x^L y + xy^U - x^L y^U. \end{aligned}$$

These constraints establish an overestimation and underestimation of the bilinear term w , which can be visualized to assess their accuracy compared to the actual bilinear relationship.



(a) Difference to the upper bound

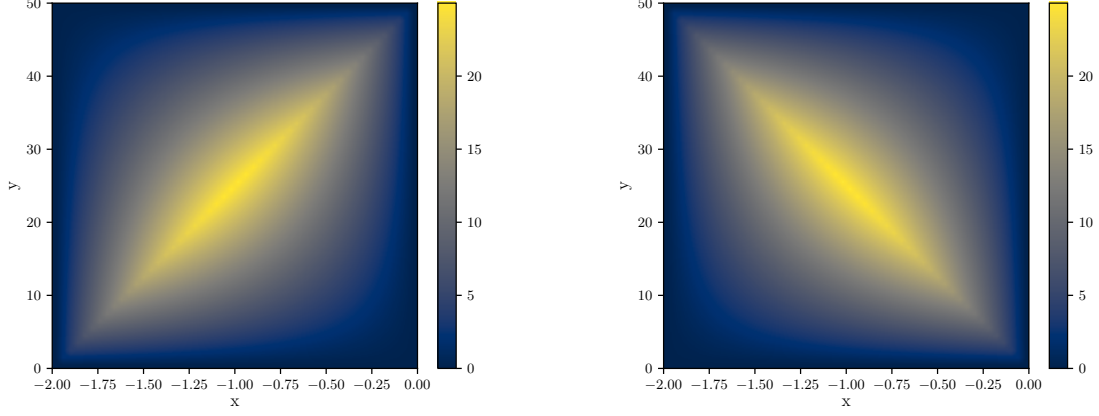


(b) Difference to the lower bound

Figure 1.1: McCormick relaxation bounds for the bilinear term $w = xy$.

Figure 1.1a illustrates the deviation between the actual bilinear term $w = xy$ and the smallest upper bound provided by the relaxation constraints. Similarly, Figure 1.1b shows

the deviation to the greatest lower bound. For the range $-2 \leq x \leq 2$ and $0 \leq y \leq 50$. It is evident that the bounds improve as x and y approach their respective limits.



(a) Difference to the upper bound

(b) Difference to the lower bound

Figure 1.2: McCormick relaxation bounds for the bilinear term $w = xy$ with stricter bounds on x .

Figures 1.2a and 1.2b present the results when x is more tightly bounded, specifically $-2 \leq x \leq 0$. One can observe that the maximum deviation is considerably reduced compared to the previous scenario, indicating that tighter bounds yield a more accurate relaxation.

To illustrate the application of these relaxations in practice, consider a path-planning scenario with $v_{min} = 1$, $v_{max} = 4$, and $v_{start} = 1$. In this scenario, the bilinear term $v\xi$, which appears in the equation of motion for $\dot{n} = v \sin \xi \approx v\xi$, is approximated using McCormick relaxations.

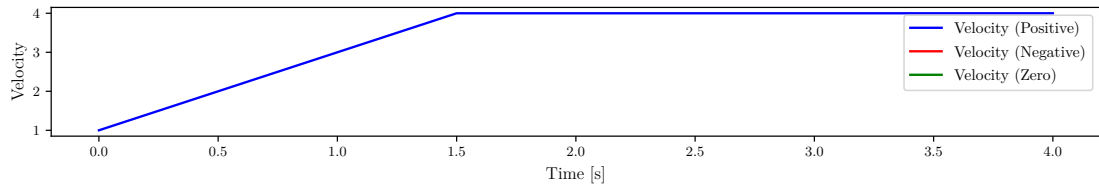


Figure 1.3: Planned velocity profile.

Figure 1.3 shows the planned velocity profile, which quickly reaches its upper limit.

Figure 1.4 depicts the alignment error ξ at each planned time point. Here, ξ is bounded within $-45^\circ \leq \xi \leq 45^\circ$. It is noteworthy that ξ does not reach these bounds.

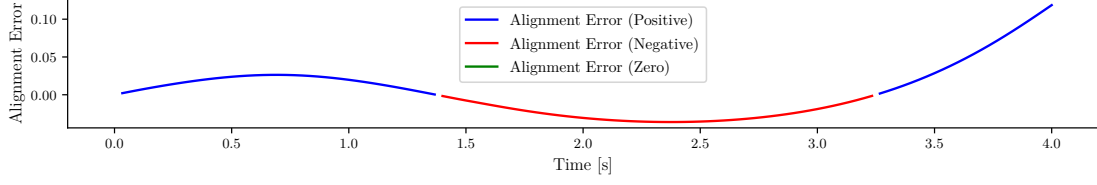


Figure 1.4: Alignment error ξ over time.

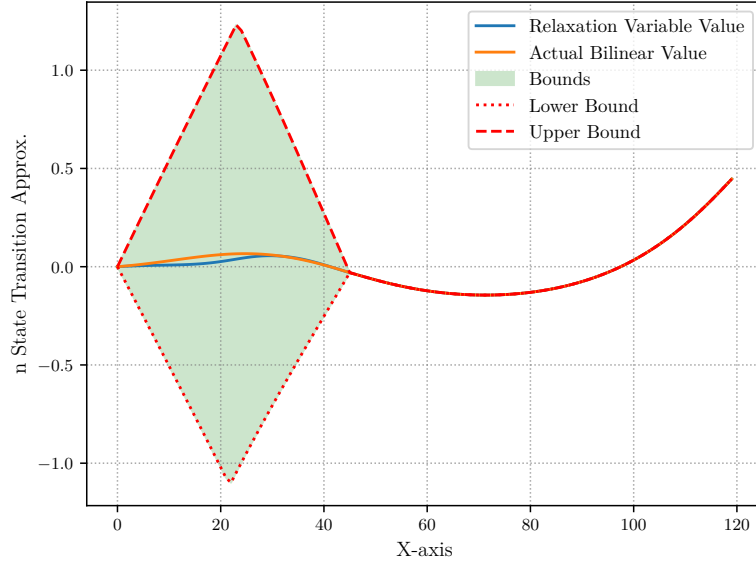


Figure 1.5: State transition approximation for n using bilinear term relaxation.

Figure 1.5 compares the actual bilinear value $v\xi$ with the relaxation variable w introduced via McCormick envelopes. This comparison highlights the accuracy of the relaxation approach in approximating the bilinear interaction and its effect on the state transition of n . Once the velocity reaches its limit, the approximation becomes increasingly accurate.

Note: The x-axis does not represent time directly but instead shows discrete time points. Here, 30 time points per second were chosen, resulting in a range from 0 to 120 for this figure, whereas the other figures range from 0 to 4.